Journal of Molecular Liquids 231 (2017) 185–191

Contents lists available at ScienceDirect

Journal of Molecular Liquids

journal homepage: www.elsevier.com/locate/molliq

Interaction between hydroxyl group and water saturated supercritical CO_2 revealed by a molecular dynamics simulation study

C. Chen [a,*], N. Zhang [b], W.J. Shen [c], W.Z. Li [a], Y.C. Song [a]

[a] Key Laboratory of Ocean Energy Utilization and Energy Conservation of Ministry of Education, Dalian University of Technology, Dalian 116024, PR China
[b] School of Petroleum and Chemical Engineering, Dalian University of Technology, Panjin 124221, PR China
[c] Key Laboratory for Mechanics in Fluid Solid Coupling Systems, Institute of Mechanics, Chinese Academy of Sciences, Beijing 100190, PR China

ARTICLE INFO

Article history:
Received 6 January 2017
Received in revised form 22 January 2017
Accepted 2 February 2017
Available online 3 February 2017

Keywords:
Hydrogen bond
Supercritical CO_2
Molecular dynamics simulation
Physi-sorption

ABSTRACT

Molecular dynamics simulations were performed to investigate hydroxyl groups-CO_2 interactions. Three silica surfaces with different hydroxyl group structures were selected and the effect of pressure was studied in the range of 4.8–32.6 MPa. Radial distribution functions especially for O_s—O_c pair show evidence for hydrogen bonds between hydroxyl groups and CO_2 molecules. The hydrogen bonds structure was analyzed using the mean number of hydrogen bonds. Pressure and hydroxyl group structures were found to affect H-bonding structure. These findings provide new insight for CO_2-hydroxyl group interactions to better understand the effects of CO_2 in carbon capture and sequestration process.

1. Introduction

The current high levels of CO_2 in the atmosphere motivate the efforts to mitigate global climate changes to decrease anthropogenic greenhouse gas emissions into the atmosphere. CO_2 capture and sequestration (CCS) is considered as one of the most promising options [1,2]. A knowledge of CO_2-solid interactions is critical for the design of improved CCS technology.

Sorption of CO_2 on solid surfaces has been the subject of many experimental and simulation studies: silica [3–9], montmorillonite [10,11], shale [12] and kaolinite [13]. We focus on CO_2 sorption on silica. The isotherms of CO_2 sorption on silica found in former studies revealed that the sorption of CO_2 strongly depended on the degree of silica surface hydroxylation [7]. Thus, the sorption of CO_2 on silica surface should be related with CO_2-hydroxyl group interaction.

It has been found that the interaction between CO_2 and hydroxyl group was so special that CO_2 was incorporated into the interparticle regions attributed to the location of the inaccessible groups [14]. To investigate the sorption mechanism, the interaction between CO_2 and hydroxyl group on silica surfaces were studied using experimental and simulation methods. Three mechanisms were proposed: (1) The weak physi-sorption mechanism. Infrared spectroscopy was used to probe the interaction of CO_2 with silica and spectra of deuterated silica immersed in supercritical CO_2 showed a weak physi-sorption with the surface silanols [15]. (2) The sorption of CO_2 on silica surface was due to the formation of hydrogen bond between the surface hydroxyls and CO_2 oxygen atoms. Using molecular dynamics (MD) simulation methods, the density profiles, radial distribution functions as well as the interfacial dynamics properties for the confined CO_2 fluid have been simulated and it was demonstrated that the hydroxylated silica surface gave a stronger confining effect on the supercritical CO_2 fluid as compared with the silylated surface which were attributed to the H-bonding interaction between the CO_2 molecules and surface hydroxyl groups [16]. Study of the interaction of CO_2 oxygen atoms with protons of muscovite hydroxyls revealed that the O—H distribution function formed a small but distinct peak at 1.8 Å, which was a clear sign of a hydrogen bond [17]. (3) A combination of physi-sorption and a weakly bonding interaction. The separate contribution of the dispersive and the quadrupole interactions to the adsorption energy were analyzed and a weakly bonded adduct was found between H atom of hydroxyl group and O atom of CO_2 [18].

Based on results of these studies, CO_2 can physically adsorb onto silica surface. Although several authors claimed that the sorption of CO_2 on silica surface was due to the formation of hydrogen bond between the surface hydroxyls and CO_2 oxygen atoms, they never analyzed the

* Corresponding author.
E-mail address: congchen@dlut.edu.cn (C. Chen).

http://dx.doi.org/10.1016/j.molliq.2017.02.008
0167-7322/

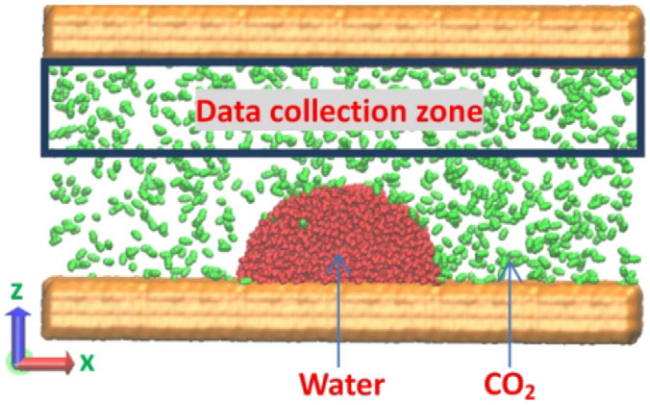

Fig. 1. The snapshot of one sample simulation box. The water droplet was placed to make sure CO_2 was fully saturated with water when system is equilibrated.

details of hydrogen bonds [7,18]. In the present study, the hydrogen bonding network was investigated using molecular dynamics simulation methods to better understand the interaction between supercritical CO_2 and hydroxyl groups.

2. Methods

2.1. System construction

Water is present in saline aquifers before supercritical CO_2 is injected in. At equilibrium, water is saturated with supercritical CO_2, while, CO_2 is also saturated with water. To mimic the equilibrium status under geologic sequestration conditions, the simulation system should be constructed with triple phases as mineral, water and CO_2. So, the simulation system was constructed following the methods which have been applied to predict contact angles [19]. The snapshot of one simulation box is illustrated in Fig. 1. The interface between the top silica surface and the water saturated CO_2 was used to analyze saturated CO_2-silica interaction.

Three silica surfaces with different terminations were selected namely Q^2, crystalline Q^3 and amorphous Q^3. A unit cell of alpha-quartz was selected to create Q^2 silica surfaces on the {0 0 1} plane with an area density of SiOH groups of 9.4/nm^2. The unit cell and the Q^2 surface are shown in Fig. 2. A unit cell of alpha-cristobalite was used to create crystalline Q^3 surfaces on the {2 0 −2} plane with an area density of SiOH groups of 4.7/nm^2. The amorphous Q^3 surface was adapted from Materials Studio and it contains some Q^2 and —SiOSi-environments with a total of 4.7 SiOH groups per nm^2. The crystalline and amorphous Q^3 surfaces are shown in Fig. 3. The parameters of simulation boxes are summarized in Table 1.

2.2. Force fields and simulation details

A force field optimized for simulating interfacial properties of silica with different functional groups was selected to describe the interactions of silica and a flexible SPC water model coupled with silica force field was used [20]. The potential energies of CO_2 molecules were calculated by a fully flexible force field [21] which was modified based on a semi-flexible EPM2 model [22]. The interaction parameters between unlike atoms were calculated using the Lorentz-Berthelot combing rules.

All simulations were performed using package NAMD [23]. Periodic boundary conditions were applied in all dimensions. Nonbonded Lennard-Jones (LJ) interactions were calculated using neighborhood and switching function cutoff techniques. The switching process was operated between 10.0 and 12.0 Å with a cutoff of 13.5 Å. The Coulombic potential was split into short-range and long-range interactions using a cutoff of 13.5 Å. The long-range Coulombic interaction was calculated by a Particle mesh Ewald (PME) method [24] using a cubic PME interpolation order with a direct sum tolerance of 10^{-6}. The PME grid sizes in three dimensions were selected based on grid spaces which were about 1.0 Å. To improve computational efficiency and also prevent

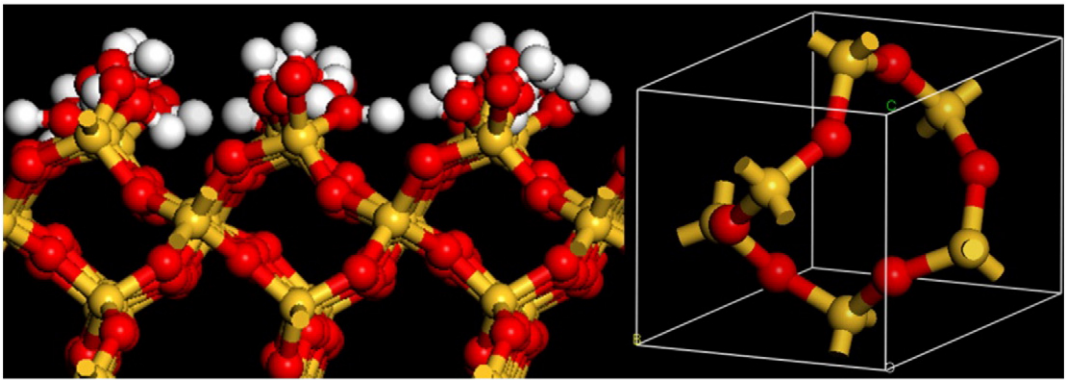

Fig. 2. The Q^2 surface (left) and the unit cell (right) of alpha-quartz used to generate the Q^2 surface.

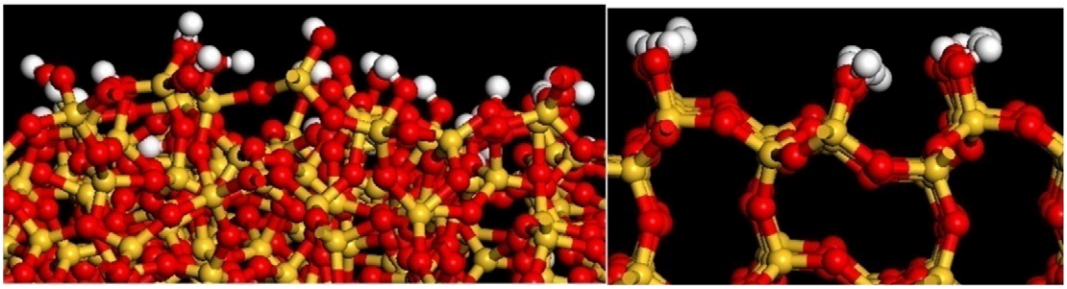

Fig. 3. The amorphous (left) and crystalline (right) Q^3 surfaces.

Table 1
Parameters of simulation boxes. p is system pressure (MPa). N_c and N_w are the numbers of CO_2 and water molecules, respectively. L_x, L_y and L_z are dimensions in x, y and z directions (nm), respectively.

p	N_C	N_w	L_x	L_y	L_z
Q^2 surface					
5	823	2085	20.95	3.47	11.66
6.1	1073	2085	20.95	3.47	11.66
8.6	1388	2085	20.95	3.51	11.66
26.4	4571	2085	20.96	3.51	11.66
32.6	5137	2085	21.20	3.72	11.66
Crystalline Q^3 surface					
5.4	793	2085	20.30	3.48	12.99
6.4	1020	2085	20.20	3.48	12.99
8.1	1337	2085	20.02	3.51	12.99
18.6	3307	2085	20.06	3.51	12.99
32.4	4874	2085	20.18	3.72	12.99
Amorphous Q^3 surface					
4.8	990	2568	20.30	4.29	12.83
5.9	1223	2473	20.31	4.50	12.89
11.7	2530	2085	20.33	4.39	13.17
14.5	3103	2085	20.33	4.39	13.19
23.2	7011	2608	20.15	4.15	12.43

unphysical oscillation of the mineral slab, atoms in minerals except for those in hydroxyl groups were held fixed during simulations using the SHAKE algorithm [25]. A multiple time steps integration technique r-RESPA [26] was adopted to calculate nonbonded LJ interaction and short-range Coulombic potential at each time step while calculating long-range Coulombic potential at every two time steps. All MD simulations were conducted in NVT ensembles after simulation boxes construction. A Langevin dynamics method with a damping coefficient of 5/ps was used to maintain temperature at 383K [27]. A total of 15 ns runs were performed with a time step of 1 fs. Data were collected from trajectory files generated in last 3 ns.

2.3. Hydrogen bonds

The geometrical criteria are usually selected to define a hydrogen bond. For a potential hydrogen bond X—H···A, the length H···A, the angle XHA and the angle HXA are frequently applied by defining a cutoff for each parameter: the length H···A is smaller than r, the angle XHA is larger than θ_1 and/or the angle HXA is smaller than θ_2. For the silica-CO_2 interaction, a possible hydrogen bond should be O_s—H_s···O_c, where O_s, H_s are the O and H atoms in a hydroxyl group and O_c is the O atom in a CO_2 molecule. The length H_s···O_c and the angle $H_sO_sO_c$ are selected to define hydrogen bonds. The cutoff of the length H_s···O_c was determined from the radial distribution functions for the atom pair H_s—O_c (Fig. 4). The cutoff of the angles $H_sO_sO_c$ was selected as 30° as used in former studies [28].

The hydrogen bonds structure at silica-CO_2 interface was analyzed using the mean number of hydrogen bonds. The percentage of O_c atoms which form i hydrogen bonds with H_s atoms is defined as $n^i(O_c)$, where i denotes 0, 1, 2 and 3. Similarly, the percentage of H_s atoms which form i hydrogen bonds with O_c atom is defined as $n^i(H_s)$. The percentage of CO_2 molecules which are involved in i hydrogen bonds is defined as $n^i(C)$. The mean number of hydrogen bonds per O_c/H_s/C can be calculated from the percentages and referred as $n(O_C)$, $n(H_s)$ and n(C), respectively.

3. Results and discussion

3.1. Radial distribution functions

Fig. 4 illustrates the radial distribution functions of different atom pairs at Q^2—CO_2, crystalline Q^3—CO_2 and amorphous Q^3—CO_2 interfaces under different pressures. Three atom pairs were analyzed namely O_s—C, O_s—O_c, H_s—O_c. One or more peaks can be found at these radial distribution functions. The peak values depend strongly on pressure. However, the peak positions show no dependence with pressure. The well structure of radial distribution functions for O_s—C pairs shows the interaction between hydroxyl groups and CO_2 molecules. The interaction may be caused by physi-sorption or hydrogen bonds [15–17]. For Q^2 and amorphous Q^3 surfaces, the first peak occurs at r = 4 Å and the first minimum is shown when r = 5.5 Å. However, the first peak position is 3.5 Å and the position for the first minimum is 5 Å at crystalline Q^3—CO_2 surface.

For the three interfaces studied, the radial distribution functions for O_s—O_c pairs get the same positions for the first peak (3.3 Å) and the first minimum (4.3 Å). The peak and minimum positions show evidence for hydrogen bonds between hydroxyl groups and CO_2 molecules [17,30]. The existence of hydrogen bonds can be further confirmed by the radial distribution functions for H_s—O_c pairs. For Q^3 surfaces (both crystalline and amorphous), the H_s—O_c distribution function forms a small but distinct peak at about 2.0 Å, which is a clear sign of a hydrogen bond [30]. The peak position of 2.0 Å is the same as that for ethanol—CO_2 hydrogen bond interaction [17,30]. However, this peak disappears on the H_s—O_c distribution function at Q^2—CO_2 interface. The hydroxyl group density at Q^2 surface is much higher than those at Q^3 surfaces and hydrogen bonds form between hydroxyl groups connected with the same Si atom [31,32]. As a result, the chances for hydroxyl groups to form hydrogen bonds with CO_2 molecules decreased which has been confirmed by hydrogen bonds analysis. In the following analysis, the position of the first minimum 4.3 Å for O_s—O_c distribution functions was selected to define hydrogen bonds between hydroxyl groups and CO_2 molecules.

3.2. Atom axial density distributions

The number densities of atoms in CO_2 molecules as a function of the distance normal to silica surface at different pressures are shown in Fig. 5. The silica surface is located at the average position of outmost Si atoms. It is clearly observed that the interfacial CO_2 molecules appear layering phenomena [16]. In all conditions studied, the number densities of C and O atoms in CO_2 molecules have the same shape but different values. The pressure has a great impact on the density profiles. The final number density far away from the silica surface increases with pressure as expected.

Near Q^2 surface, the density profile displays a peak at about 3.3 Å and the first shell ends at 5.1 Å. At high pressures, a second peak can be found about 7 Å away from the surface. However, the second peak disappears at low pressures. The peak locations for C and O atoms in CO_2 molecules are same and show no dependence on system pressure. Same results can be found by analyzing the number densities normal to crystalline Q^3 surface except that the peak values are much smaller compared with that near Q^2 surface. The situation near amorphous Q^3 surface is different. At all pressures studied, only one peak can be found, the peak location changes with pressure and the density distribution curve is much rougher. The effects of silica surface on density profiles are related with hydroxyl groups on silica surfaces. Compared with the two Q^3 surfaces, on Q^2 surface, the density of hydroxyl groups is larger leading to higher peak values. This is consistent with former studies where the attraction between hydroxylated silica and CO_2 was found to be significantly weaker compared for dyhydroxylated silica [7].

Although the density of hydroxyl groups on crystalline and amorphous Q [3] surfaces is the same, the disorder of hydroxyl group distribution causes pressure dependence of peak location. The strong peak near silica surfaces found from density profiles proves the interaction between hydroxyl groups and CO_2 molecules. The features of atom axial density distributions also imply that the interaction between hydroxyl groups and CO_2 molecules is affected by pressure and surface hydroxyl group structures. In fact, water contact angles on silica surfaces under CO_2 atmosphere were found to strongly relate with pressure

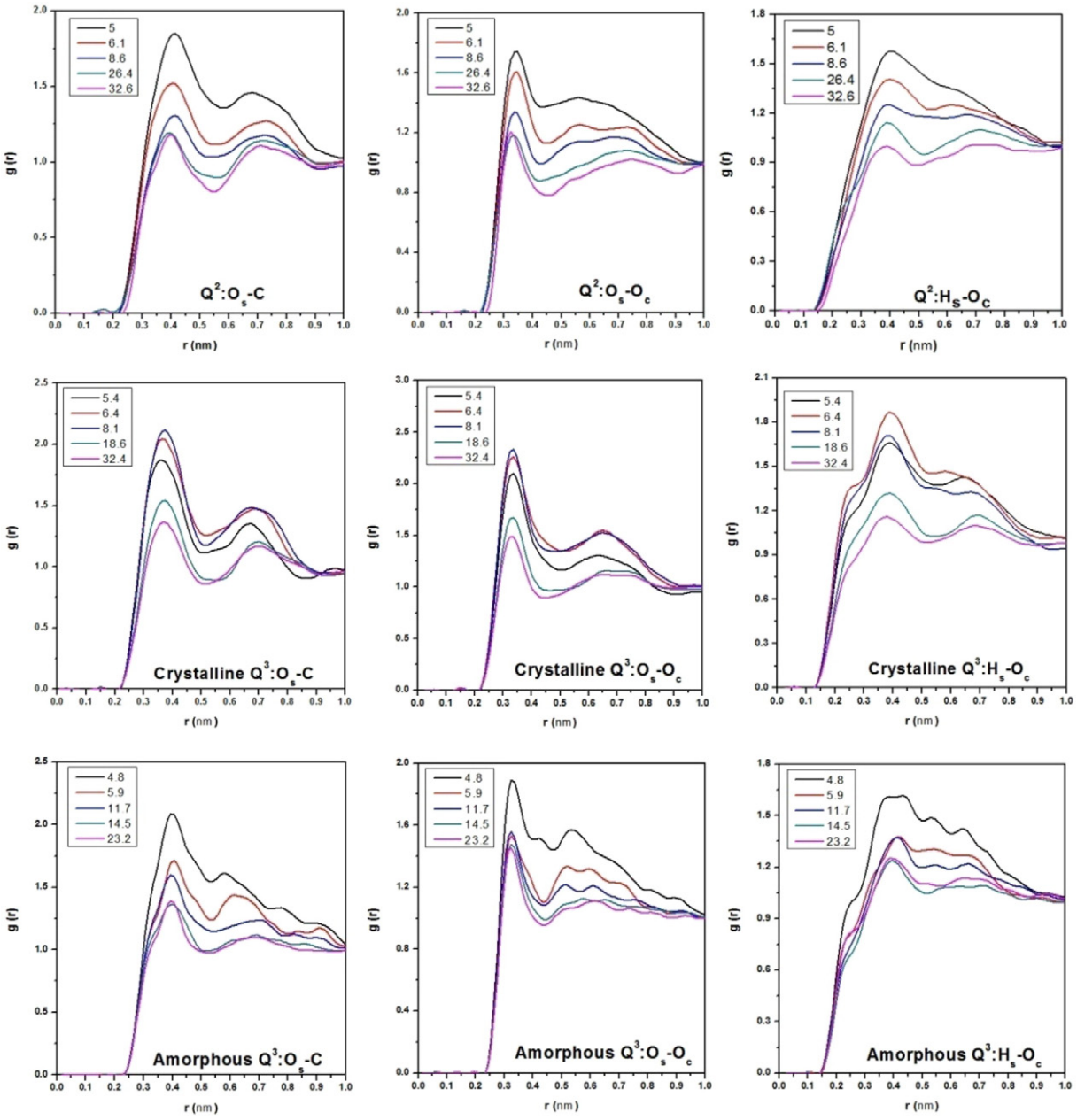

Fig. 4. The radial distribution functions of different atom pairs.

[33] as well as surface hydroxyl group density and space distribution [32].

3.3. Hydrogen bonds analysis

3.3.1. Hydrogen bonds structure of H_s atoms

Fig. 6 shows the percentage of H_s atoms which are involved in hydrogen bonds or not. Fig. 7 illustrates the mean number of hydrogen bonds per H_s atom formed with CO_2 molecules. As pressure increases, the local density of CO_2 molecules rises near silica surfaces (as seen in Fig. 5). More CO_2 molecules are present to interact with hydroxyl groups and the percentage of H_s atoms which form one hydrogen bond with CO_2 molecules becomes larger. Conversely, the percentage of H_s atoms which are not hydrogen bonded with any CO_2 molecules decreases with pressure. As a result, the mean number of hydrogen bond per H_s atom increases with pressure (Fig. 7). At each Si site of Q^2 surface, there are two hydroxyl groups which form hydrogen bonds with each other [31]. The chance of each hydroxyl group interacting with nearby CO_2 molecules decreases. On crystalline Q^3 surface, there are no hydrogen bonds formed between nearby hydroxyl groups [31] and each hydroxyl group can form hydrogen bonds with CO_2 molecules freely without the influence of nearby hydroxyl groups. On amorphous Q^3 surface, the hydroxyl group form hydrogen bonds with other hydroxyl groups although much smaller compared with that on Q^2 surface [31]. As a result, the percentage of H_s atoms forming one hydrogen bond with CO_2 molecules and the mean number of hydrogen bonds per H_s atom follow the order of crystalline Q^3 > amorphous Q^3 > Q^2. It should be noted that as only one kind hydrogen bond can be formed between hydroxyl groups and CO_2 molecules, the results for the O_s atoms are the same as that for H_s atoms.

3.3.2. Hydrogen bonds structure of O_c atoms

To analyze the hydrogen bond structure of O_c atoms, we focus on O_c atoms which are located within the first hydration shell of O_s atoms

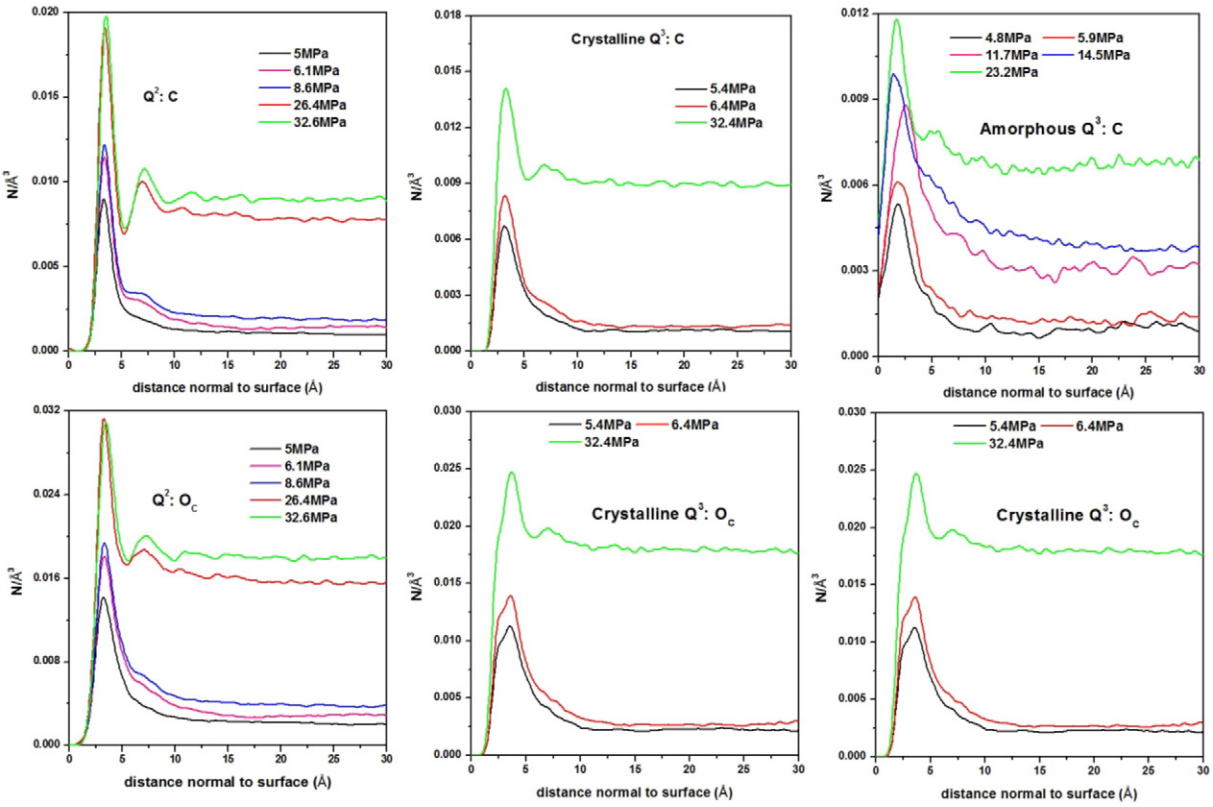

Fig. 5. The number densities of atoms in CO_2 molecules as a function of the distance normal to silica surface at different pressures.

(4.3 Å away from the O_s atoms, Fig. 4). The percentage of O_c atoms which form different numbers of hydrogen bonds is illustrated in Fig. 8. The mean number of hydrogen bonds per O_c atom formed with hydroxyl groups is summarized in Fig. 9. As pressure increases, the percentage of O_c atoms which form one hydrogen bond with hydroxyl groups on crystalline Q^3 surface decreases leading to decrease of mean number of hydrogen bonds per O_c atom. However, the effects of pressure on $n^i(O_c)$ and $n(O_c)$ are negligible for Q^2 and amorphous Q^3 surfaces. By average, 20% of O_c atoms which are located in the first hydration of shell of O_s atoms form one hydrogen bond with hydroxyl groups on silica surface.

3.3.3. Hydrogen bonds structure of CO_2 molecules

To analyze the interaction between hydroxyl groups and CO_2 molecules from the viewpoint of CO_2 molecules, we focus on CO_2 molecules of which at least one O_c atom is located within the first hydration shell of O_s atoms. Among these CO_2 molecules, those form hydrogen bonds with hydroxyl groups are classified as hydrogen bonds CO_2 molecules and the others are classified as physi-sorption CO_2 molecules.

Fig. 10 illustrates the percentage of CO_2 molecules which are involved in 0, 1 or 2 hydrogen bonds as a function of pressure on different silica surfaces. For Q^2 and amorphous Q^3 surfaces, the percentages show no dependence on pressure. For Q^2 surface, the percentage of CO_2

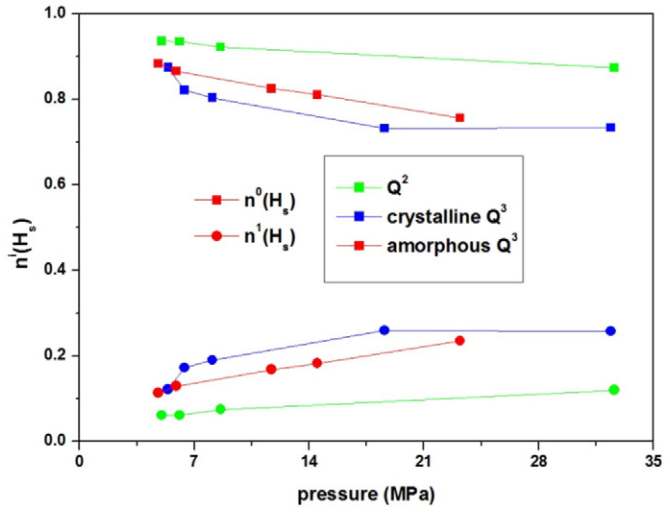

Fig. 6. The percentage of H_s atoms which are involved in 0 or 1 hydrogen bond as a function of pressure on different silica surfaces.

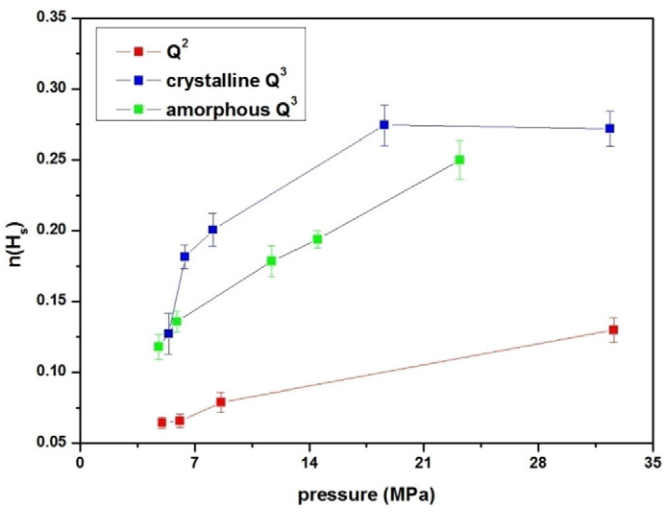

Fig. 7. The mean number of hydrogen bonds per H_s atom as a function of pressure on different silica surfaces.

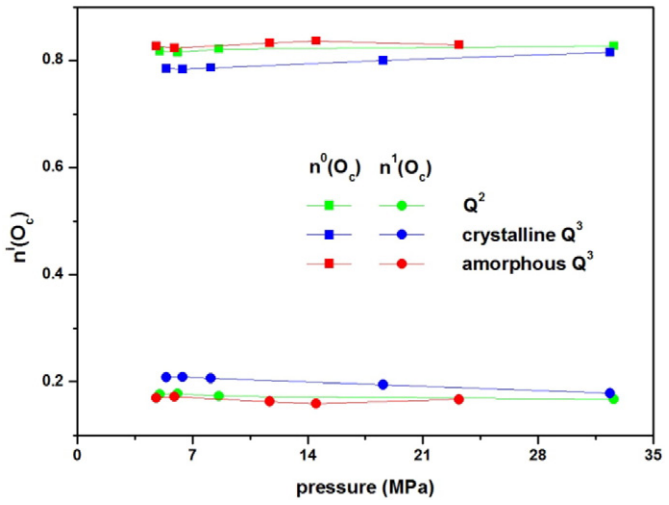

Fig. 8. The percentage of O_c atoms which are involved in 0 or 1 hydrogen bond as a function of pressure on different silica surfaces.

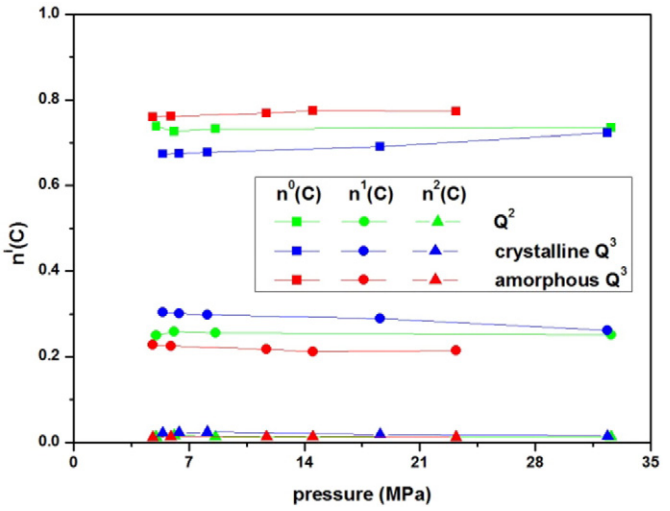

Fig. 10. The percentage of CO_2 molecules which are involved in 0, 1 or 2 hydrogen bonds as a function of pressure on different silica surfaces.

molecules that form one hydrogen bond is ~25.4% and about 1.4% of CO_2 molecules are involved with two hydrogen bonds. The rest 73.2% of CO_2 molecules are physi-sorption CO_2 molecules. For amorphous Q^3 surface, the percentage of physi-sorption CO_2 molecules is 76.7%. 22% and 1.3% of CO_2 molecules are involved with one and two hydrogen bonds, respectively. The results for crystalline Q^3 surface are different. As pressure rises from 5.4 to 32.4 MPa, the percentage of physi-sorption CO_2 molecules increases from 67.4% to 72.3%. The decrease of percentage of hydrogen bonds CO_2 molecules is caused mainly by loss of CO_2 molecules which form only one hydrogen bond with hydroxyl groups (dropping from 30% to 26%). In summary: for Q^2 and amorphous Q^3 surfaces, the percentages of physi-sorption and hydrogen bonds CO_2 molecules remain constant as pressure increases; for crystalline Q^3 surface, the percentage of physi-sorption CO_2 molecules increases with pressure. These trends are consistent with the mean number of hydrogen bonds per CO_2 molecule as drawn in Fig. 11. Each CO_2 molecule forms 0.28 hydrogen bonds with hydroxyl groups on Q^2 surface. The number reduces to 0.245 when the surface changes to amorphous Q^3. On crystalline Q^3 surface, the mean number of hydrogen bonds per CO_2 molecule decreases from 0.35 to 0.29 dropping about 17%.

4. Conclusions

Molecular dynamics simulations have been performed to investigate hydroxyl groups-CO_2 interactions. Three silica surfaces with different hydroxyl group structures were selected and the effect of pressure was studied in the range of 4.8–32.6 MPa. Radial distribution functions and atom axial density distributions have been calculated and their features show that the interaction between hydroxyl groups and CO_2 molecules is affected by pressure and surface hydroxyl structures. Radial distribution functions especially for O_s—O_c pair show evidence for hydrogen bonds between hydroxyl groups and CO_2 molecules.

Each H_s atom at most forms one hydrogen bond with CO_2 molecules. Based on pressure and surface hydroxyl group structures, 6.2%–26% of H_s atoms are involved in hydrogen bonds corresponding to 0.06–0.27 hydrogen bonds per H_s atom. For O_c atoms which are located within the first hydration shell of O_s atoms, 15.9%–20.9% are forming one hydrogen bond with surface hydroxyl groups leading to 0.17–0.22 hydrogen bonds per O_c atom. The mean number of hydrogen bonds per H_s atom formed between hydroxyl group and CO_2 molecules follows the order as crystalline Q^3 > amorphous Q^3 > Q^2. For Q^2 and amorphous Q^3 surfaces, the pressure shows negligible effect on the percentage of

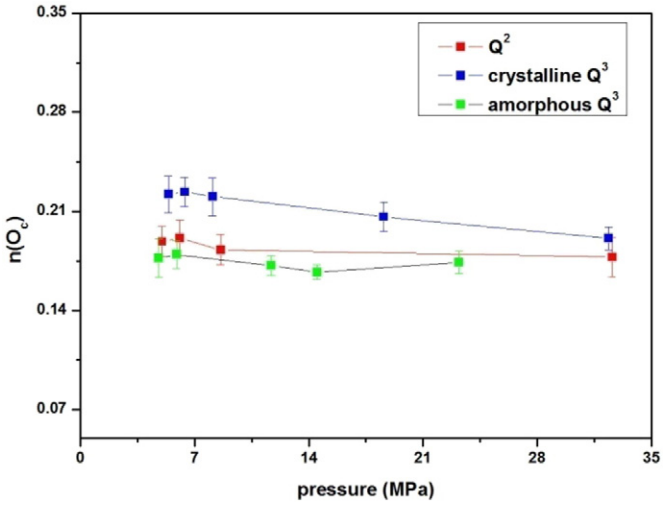

Fig. 9. The mean number of hydrogen bonds per O_c atom as a function of pressure on different silica surfaces.

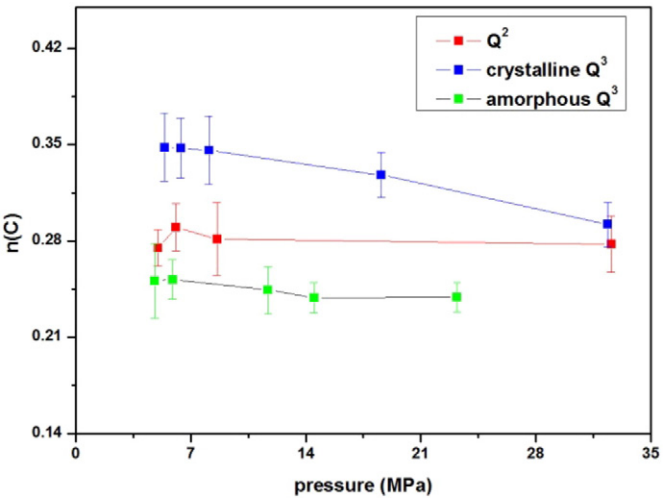

Fig. 11. The mean number of hydrogen bonds per CO_2 molecule as a function of pressure on different silica surfaces.

O_c atoms which are involved in 0 or 1 hydrogen bond as well as the mean number of hydrogen bonds per O_c atom. However, the percentage of O_c atoms which form one hydrogen bond with hydroxyl groups on crystalline Q^3 surface decreases with pressure leading to decrease of mean number of hydrogen bonds per O_c atom. The mean number of hydrogen bonds per O_c atom for crystalline Q^3—CO_2 hydrogen bond is the largest.

CO_2 molecules of which at least one O_c atom is located within the first hydration shell of O_s atoms were classified as hydrogen bonds CO_2 molecules and physi-sorption CO_2 molecules. The percentages of physi-sorption CO_2 molecules for Q^2 and amorphous Q^3 surfaces show no dependence with pressure with values of 73.2% and 76.7%, respectively. For crystalline Q^3 surface, the percentage of physi-sorption CO_2 molecules increases from 67.4% to 72.3% when pressure increases from 5.4 to 32.4 MPa. It's interesting that the percentage of physi-sorption CO_2 molecules for crystalline Q^3 surface is the smallest and the value for amorphous Q^3 surface is the largest.

These findings provide new information to better understand the interaction between supercritical CO_2 and mineral surfaces. The knowledge of CO_2-mineral interaction is essential to investigate wettability of CO_2/brine/mineral systems which is a key parameter to govern the fate of supercritical CO_2 during CCS. However, further studies are required to construct direct relationship between CO_2-mineral hydrogen bonds interaction and CO_2-mineral interfacial tension.

Acknowledgements

This research was supported by National Natural Science Foundation of China (51206016 and 51676027), Natural Science Foundation of Liaoning Province (201602147) and the Fundamental Research Funds for the Central Universities (DUT14LAB13).

References

[1] K. Michael, A. Golab, V. Shulakova, J. Ennis-King, G. Allinson, S. Sharma, T. Aiken, Int, J. Greenhouse Gas Control 4 (2010) 659–667.
[2] L.M. Hamm, I.C. Bourg, A.F. Wallace, B. Rotenberg, in: D.J. DePaolo, D.R. Cole, A. Navrotsky, I.C. Bourg (Eds.), Geochemistry of Geologic CO_2 Sequestration, vol. 77, Mineralogical Soc Amer, Chantilly 2013, pp. 189–228.
[3] Y.F. He, N.A. Seaton, Langmuir 19 (2003) 10132–10138.
[4] V.A. Bakaev, W.A. Steele, T.I. Bakaeva, C.G. Pantano, J. Chem. Phys. 111 (1999) 9813–9821.
[5] C.G. Sonwane, S.K. Bhatia, N. Calos, Ind. Eng. Chem. Res. 37 (1998) 2271–2283.
[6] K. Morishige, H. Fujii, M. Uga, D. Kinukawa, Langmuir 13 (1997) 3494–3498.
[7] A. Vishnyakov, Y.Y. Shen, M.S. Tomassone, J. Chem. Phys. 129 (2008) 174704.
[8] M.D. Elola, J. Rodriguez, J. Phys. Chem. C 120 (2016) 1262–1269.
[9] O. Di Giovanni, W. Dorfler, M. Mazzotti, M. Morbidelli, Langmuir 17 (2001) 4316–4321.
[10] A. Kadoura, A.K.N. Nair, S.Y. Sun, Microporous Mesoporous Mater. 225 (2016) 331–341.
[11] M.M. Sena, C.P. Morrow, R.J. Kirkpatrick, M. Krishnan, Chem. Mater. 27 (2015) 6946–6959.
[12] S. Duan, M. Gu, X.D. Du, X.F. Xian, Energy Fuel 30 (2016) 2248–2256.
[13] Y.H. Chen, D.L. Lu, Appl. Clay Sci. 104 (2015) 221–228.
[14] B. McCool, C.P. Tripp, J. Phys. Chem. B 109 (2005) 8914–8919.
[15] C.P. Tripp, J.R. Combes, Langmuir 14 (1998) 7350–7352.
[16] Y. Qin, X. Yang, Y. Zhu, J. Ping, J. Phys. Chem. C 112 (2008) 12815–12824.
[17] D.R. Cole, A.A. Chialvo, G. Rother, L. Vlcek, P.T. Cummings, Philos. Mag. 90 (2010) 2339–2363.
[18] R. Roque-Malherbe, R. Polanco-Estrella, F. Marquez-Linares, J. Phys. Chem. C 114 (2010) 17773–17787.
[19] C. Chen, B. Dong, N. Zhang, W. Li, Y. Song, Energy Fuel 30 (2016) 5027–5034.
[20] F.S. Emami, V. Puddu, R.J. Berry, V. Varshney, S.V. Patwardhan, C.C. Perry, H. Heinz, Chem. Mater. 26 (2014) 2647–2658.
[21] L. Vlcek, A.A. Chialvo, D.R. Cole, J. Phys. Chem. B 115 (2011) 8775–8784.
[22] J.G. Harris, K.H. Yung, J. Phys. Chem. 99 (1995) 12021–12024.
[23] J.C. Phillips, R. Braun, W. Wang, J. Gumbar, E. Tajkhorshid, E. Villa, C. Chipot, R.D. Skeel, L. Kale, K. Schulten, J. Comput. Chem. 26 (2005) 1781–1802.
[24] T. Darden, D. York, L. Pedersen, J. Chem. Phys. 98 (1993) 10089.
[25] J.P. Ryckaert, Mol. Phys. 55 (1985) 549–556.
[26] P. Procacci, M. Marchi, J. Chem. Phys. 104 (1996) 3003.
[27] A.T. Brunger, A System for X-ray Crystallography and NMR, 1992 (Journal).
[28] C. Chen, W.Z. Li, Y.C. Song, J. Yang, J. Mol. Liq. 146 (2009) 23–28.
[30] M. Saharay, S. Balasubramanian, J. Phys. Chem. B 110 (2006) 3782–3790.
[31] C. Chen, N. Zhang, W. Li, Y. Song, Mol. Phys. (2016) 1–12.
[32] C. Chen, N. Zhang, W. Li, Y. Song, Environ. Sci. Technol. 49 (2015) 14680–14687.
[33] A.L. Benavides, J.L. Aragones, C. Vega, J. Chem. Phys. (2016) 144.